COBEM 2021 Florianópolis - Brasil
ABCM Associação Brasileira de Engenharia e Ciências Mecânicas
26th ABCM International Congress of Mechanical Engineering
November 22-26, 2021. Florianópolis, SC, Brazil

COB-2021-0492
CHAOS IN A SPATIOTEMPORAL DUFFING-TYPE SYSTEM

Eduardo V. M. dos Reis
Marcelo A. Savi
Universidade Federal do Rio de Janeiro, COPPE, Department of Mechanical Engineering, Center for Nonlinear Mechanics
eduardovillela@mecanica.coppe.ufrj.br
savi@mecanica.coppe.ufrj.br

Abstract. *Spatiotemporal dynamics arises in systems that are governed by partial differential equations. Complex dynamics is expected for nonlinear systems and spatiotemporal chaos is an emblematic example of this complexity. The Navier-Stokes, Ginzburg-Landau and Kuramoto-Sivashinsky are some examples of complex nonlinear spatiotemporal systems. Several physical phenomena define the system behavior including diffusion, convection and energy generation. This paper deals with the investigation of spatiotemporal chaos on a conservative Duffing-type system. Finite Difference and the fourth-order Runge-Kutta methods are employed for numerical discretization. A conservative system is of concern which means that mechanical energy is preserved through time. Results show a correlation between the space perturbation magnitude growth and the system Hamiltonian .*

Keywords: *Mechanical vibration, Spatialtemporal chaos, Duffing system, Chaos.*

1. INTRODUCTION

The study of spatiotemporal chaos has an increasing relevance in science and engineering, being a challenging topic. Several scientific problems can be modeled with spatial dependence, such as chemistry, optics and mechanics (Merkin *et al.*, 1996; Guzmán and Amon, 1994; Elder *et al.*, 1997). Reis *et al.* (2018) studied nonlinear dynamics of a sea pipeline showing that vibration induced by sea flow can be treated by both linear and nonlinear approaches. The Generalized Integral Transform Technique was employed showing good computational efficiency. Fang *et al.* (2017a) studied nonlinear acoustic metamaterial, focusing on diatomic and a tetratomic meta unit-cell. Wave attenuation was investigated showing that nonlinear effects can significantly expand the bandwidth for elastic wave suppression.

Spatiotemporal chaos is another correlated subject that can be found in the literature (Hill, 1992; Yang and Chen, 2005; Gotoda *et al.*, 2015). The evolution of chaos in the space-time domain is an interesting topic of research due to engineering applications. Deissler and Kaneko (1987) investigated an open flow system modeled by the Ginzburg-Landau equation, defining a measure for chaos using Lyapunov exponent with velocity dependence. Deissler (1987) studied spatially growing wave and convective chaos. Wackerbauer and Showalter (2003) analyzed the the collapse of spatiotemporal chaos in reaction-diffusion systems.

Systems given by a chain of coupled oscillators is employed to model several physical systems. Umberger *et al.* (1989) was one of the pioneer work studying a chain of Duffing oscillators considering periodic boundary conditions and observing pattern formation when the system undergoes harmonic excitation. Musielak *et al.* (2005) studied routes to chaos in a network of Duffing oscillators, showing that the increase of the number of degrees of freedom can lead to crisis, instead of period doubling, as the main route to chaos. Romeo and Rega (2006) carried out an analysis of wave propagation in a chain of Duffing oscillators. Metamaterial is another class of periodic structures modeled by an oscillator network (Fang *et al.*, 2017b).

This paper investigates the spatiotemporal chaos in a Duffing-type system governed by a partial differential equation (PDE), which is equivalent to a network of Duffing Oscillators (Umberger *et al.*, 1989). This system can represent a network of Moon beams (Moon and Holmes, 1979) coupled by linear springs. The effect of dissipation and external excitation are neglected and, therefore, a Hamiltonian system is carried out. The dynamical analysis considers a space split treating space and time separately. Dynamical analysis is treated from perturbation analysis and an energetic approach is also employed for dynamical investigation. Some mathematical tools are defined in order to quantify the spatiotemporal chaos. It was demonstrated that the rate of the perturbation growth in time depends on the mechanical energy of the Duffing-type system.

2. SPATIOTEMPORAL DUFFING-TYPE SYSTEM

Consider a Duffing-type system that presents a restoring force described by a cubic nonlinear polynomial, governed by PDE presented in the sequence by considering the dimensionless variables: u represents the longitudinal displacement, x is the spatial coordinate in such a way that $x \in [0,1]$ and t is the time.

$$\ddot{u} = \sigma u'' + \sigma' u' + \frac{1}{2}\left(u - u^3\right) \; ; \qquad \text{with boundary condition: } \; u(0,t) = u(1,t) = 0 \tag{1}$$

where $\dot{(\,)}$ means partial time derivative $\partial/\partial t$ and $(\,)'$ denotes spatial partial derivative $\partial/\partial x$; $\sigma = \sigma(x)$ is a spatial coupling coefficient which means that the system is spatial decoupled when $\sigma = 0$. Under this assumption, the system presents three equilibrium configurations: $u\,(\text{stable}) = -1$, $u\,(\text{unstable}) = 0$ and $u\,(\text{stable}) = 1$. Therefore, displacements $u = -1$ and $u = 1$ are considered well positions. On the other hand, in the limit $\sigma \to \infty$, there is a rigid attachment with only one possible solution: $u(x,t) = 0$. It is worthwhile mentioning that stiffness gradient $\sigma'(x)$ leads to an asymmetry of wave propagation in the spatial direction.

In order to write the system in the canonical form, the system is rewritten as a first order system as follows:

$$\begin{aligned} &\dot{u} = v \,, \\ &\dot{v} = \sigma u'' + \sigma' u' + \frac{1}{2}(u - u^3) \,; \\ &\text{with} \;\; u(0,t) = u(1,t) = 0 \end{aligned} \tag{2}$$

System integration can be achieved by considering the second order finite difference scheme for spatial discretization while time discretization is performed with fourth order Runge-Kutta method.

2.1 PERTURBATION ANALYSIS

A general form of the dynamical system with spatial dependence can be written as $\dot{\mathbf{u}} = f(\mathbf{u}, \mathbf{u}', \mathbf{u}'', \mathbf{u}''', ..., \mathbf{u}^{(n)}, \mathcal{P})$, where $\mathbf{u} \in \Re^n$ and $\mathcal{P}$ represents a set of parameters.

Let $\widehat{\mathbf{u}}$ be a reference solution of the equation of motion. One can linearize Eq. 1 around this reference solution giving rise to a perturbation equation that describes the time evolution of a perturbed orbit. Therefore, it is possible to define equations of motion for the reference and the perturbed orbits,

$$\dot{\widehat{\mathbf{u}}} = f(\widehat{\mathbf{u}}, \mathcal{P}) \tag{3a}$$

$$\dot{\mathbf{u}}_p = \left.\frac{\partial f}{\partial \mathbf{u}}\right|_{\widehat{\mathbf{u}}} \mathbf{u}_p + \sum_{i=1}^{n} \left.\frac{\partial f}{\partial \mathbf{u}^{(i)}}\right|_{\widehat{\mathbf{u}}^{(i)}} \mathbf{u}_p^{(i)} \tag{3b}$$

Perturbed orbit evolution defines the main characteristic of the system dynamics. Note that an increasing of the perturbation magnitude through time shows the sensitivity of the reference orbit $\widehat{\mathbf{u}}$ to perturbations, which characterize chaos. On the other hand, a convergence between both orbits characterizes a periodic solution.

In order to quantify the perturbation growth one defines a quantity, Ψ, that stands for the evolution throughout time of the average of the perturbation in the spatial domain. Chaotic situations present a growing Ψ, as for periodic solutions are characterized by a asymptotic decrease of Ψ. Following, it is defined as follows

$$\Psi(t) = \sqrt{\frac{\int_V \langle \mathbf{u}_p(\mathbf{x},t), \mathbf{u}_p(\mathbf{x},t) \rangle \, \mathrm{d}\mathbf{v}}{\int_V \langle \mathbf{u}_p(\mathbf{x},0), \mathbf{u}_p(\mathbf{x},0) \rangle \, \mathrm{d}\mathbf{v}}} \tag{4}$$

where $\langle \, \rangle$ yields inner product and V is the whole spatial domain. It is worthwhile mentioning that the presented definition of Ψ stands for the integral of the perturbation vector over all the spatial domain. This parameter does not give any information about the spatial distribution of the perturbation. Instead, one needs to evaluate $\phi(\mathbf{x},t)$ if seeking its spatial distribution, which is given as follows

$$\phi(\mathbf{x},t) = \sqrt{\langle \mathbf{u}_p(\mathbf{x},t), \mathbf{u}_p(\mathbf{x},t) \rangle} \tag{5}$$

Therefore, the perturbed orbit is carried out employing both Ψ and ϕ. Specifically for the problem carried out herein given by Eq. 2, Ψ as defined for a spatial system by Eq. 4, it is defined for this system as follows

$$\Psi(t) = \sqrt{\frac{\int_0^1 u_p(x,t)^2 + v_p(x,t)^2 \, \mathrm{d}x}{\int_0^1 u_p(x,0)^2 + v_p(x,0)^2 \, \mathrm{d}x}} \tag{6}$$

In order to investigate the spatial perturbation distribution and evolution, the parameter ϕ is herein considered as

$$\phi(x,t) = \sqrt{u_p(x,t)^2 + v_p(x,t)^2} \tag{7}$$

2.2 CONSERVATION OF MECHANICAL ENERGY

Energy conservation can be established by integrating governing equation during a time interval $[t_1, t_2]$ over the whole spatial domain $[0, 1]$. Therefore, it is possible to write

$$\int_0^1 \int_{t_1}^{t_2} \left[-\ddot{u} + \sigma u'' + \sigma' u + \left(\frac{u}{2} - \frac{u^3}{2} \right) \right] \dot{u} \, \mathrm{d}t \, \mathrm{d}x = 0 \tag{8}$$

After integration by parts and some algebraic manipulation, one finally obtains the energy balance equation or, in other words, the conservation of mechanical energy, as given by Eq. 9.

$$\left[\int_0^1 \left(\frac{1}{2} v^2 + \frac{1}{2} \sigma \left(\frac{\partial u}{\partial x} \right)^2 - \frac{1}{4} u^2 + \frac{1}{8} u^4 \right) \mathrm{d}x \right]_{t_1}^{t_2} = 0 \tag{9}$$

Since the numerical value from the integral between brackets in Eq.9 must be the same at any given time instants t_1 and t_2, it implies that this value must be a constant throughout time. This is a characteristic of Hamiltonian systems. Also, according to classical mechanics, this value is called mechanical energy of the system, which is also the Hamiltonian of the system, and it can be written a sum of three different kinds of energy, as follows

$$\begin{aligned} &\text{Kinetic energy} \Rightarrow E_K = \int_0^1 \frac{1}{2} v^2 \, \mathrm{d}x \\ &\text{Potential energy} \Rightarrow E_P = \int_0^1 \frac{1}{2} \sigma \left(u' \right)^2 \, \mathrm{d}x \\ &\text{Duffing-type potential energy} \Rightarrow E_D = \int_0^1 \left(-\frac{1}{4} u^2 + \frac{1}{8} u^4 + \frac{1}{8} \right) \mathrm{d}x \end{aligned} \tag{10}$$

where the Hamiltonian can be defined from the energies: $H = E_K + E_P + E_D$. Note that the addition of $1/8$ to E_D is done in order to make $E_D \geq 0 \ \forall \ u(x)$ and it does not violate the conservation of mechanical energy given by Eq.9. Since E_K and E_P are always positive, the mechanical energy becomes strictly positive for any $u(x)$ and $v(x)$.

3. NUMERICAL SIMULATIONS

This section presents results of numerical simulations, being divided into two subsections: a dynamical investigation; and a perturbation analysis where the space-time evolution are evaluated from different initial Gaussian bell shaped perturbation placed at the middle of the spatial domain.

3.1 DYNAMICAL ANALYSIS

Dynamical behavior of the Duffing-type system is of concern varying the mechanical energy and fixing σ. All simulations are carried out for $\sigma = 5 \times 10^{-4}$ or otherwise if mentioned. According to Eq. 1, if $\dot{u} = 0$, one obtains the spatial equilibrium configuration. These configurations are obtained by means of the Shooting Method, since Eq. 1 is a boundary value problem. Regarding the spatiotemporal dynamical analysis, different values of the mechanical energy is of concern, defining $H = h$. Tab. 1 shows the initial conditions employed for each simulation for each value of h; where $f(x)$ represents the equilibrium configuration of the system with the lowest value of mechanical energy, whose $h = 0.0149$. Therefore, the simulation with $h = 0.015$ regards a small sine shaped perturbation around the just mentioned equilibrium configuration. Spatial discretization is obtained with 5001 points, and the time marching is performed with a time step of 5×10^{-4}. Simulations are analyzed until a time of 65×10^3.

Table 1. Initial Conditions employed.

h	Initial Condition	
	$u(x,0)$	$v(x,0)$
0.015	$f(x) + 0.0191 \sin(\pi x)$	0
0.5	$2.107 \sin(\pi x)$	0
5	$3.406 \sin(\pi x)$	0

Dynamical response is represented by considering a specific space position, x. Fig. 1 shows the time history at spatial position $x = 1/2$ and its respective frequency domain analysis. Note that for $h = 0.015$, the dynamical response is

given by the eigenmodes from the Linear Stability Analysis around $f(x)$ oscillating around it. This behavior becomes clear in the frequency domain, that transformed $(t, u(x = 1/2)) \rightarrow (\omega, A)$ by means of a Fast Fourier Transformation (FFT), where the peaks correspond to the linear eigenfrequencies. This occurs due to the small perturbation applied to the respective equilibrium configuration and its stability. For higher levels of h, the initial condition employed led to a chaotic behavior. Once again, frequency domain clearly show the spread over several frequencies. It should also be pointed out that for $h = 0.5$, the response is an intra-well oscillation, occurring around only one well of the Duffing-type potential energy. For $h = 5$, the mechanical energy is higher and therefore the system has enough energy to overcome the well energy barrier and thus presents an inter-well oscillation, around both wells.

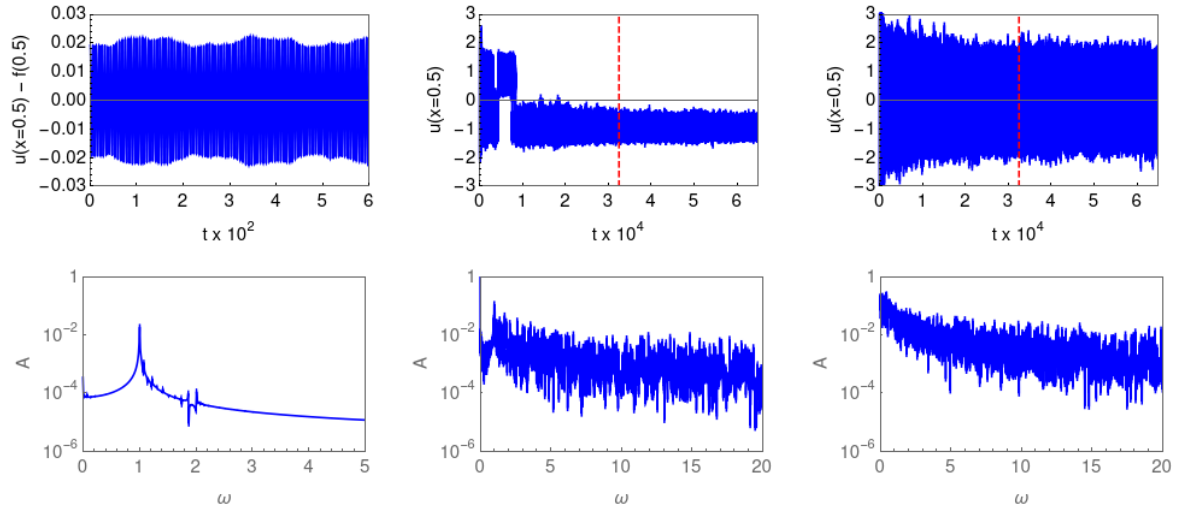

(a) $h = 0.015$ (b) $h = 0.5$ (c) $h = 5$

Figure 1. Time history and its frequency domain analysis at $x = 1/2$ for three different h values. The red lines stand for $t = 300$ (a) and $t = 325 \times 10^2$ ((b) and (c)), where the spatial analysis is performed.

Spatial analysis is performed by considering the spatially distributed displacement at a fixed time: $t = 300$ for $h = 0.015$, and $t = 325 \times 10^2$ for $h = 0.5$ and 5. When $h = 0.015$, there is a symmetry with respect to $x = 1/2$. On the other hand, the spatial configuration for $h = 0.5$ and $h = 5$ are irregular, which is a spatial chaotic behavior. Therefore, the dynamics for the situations with $h = 0.5$ and $h = 5$, are temporally and spatially irregular, characterizing a spatiotemporal chaos. The spatial frequency domain view was obtained employing also a FFT, which transformed $(x, u(t = 300)) \rightarrow (\lambda, \Lambda)$

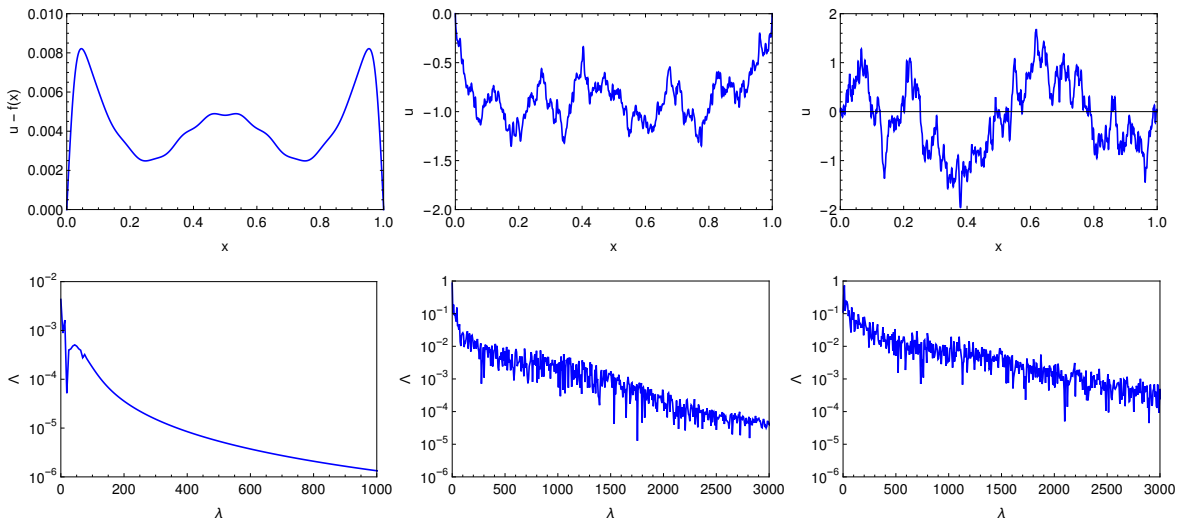

(a) $h = 0.015$ (b) $h = 0.5$ (c) $h = 5$

Figure 2. Displacement spatial configurations and its respective spatial frequency domain for three different h values.

3.2 PERTURBATION DYNAMICAL ANALYSIS

This section deals with the spatiotemporal dynamics of the perturbation around a reference response. It exploits the time evolution of Ψ and the spatiotemporal evolution of the perturbation. The perturbation initial condition is $u_p(x,0) = 2.825\,\exp\left[-100(x-1/2)^2\right]$ and $v_p(x,0) = 0$, which gives $\int_0^1 \langle \mathbf{u}_p(\mathbf{x},t), \mathbf{u}_p(\mathbf{x},t)\rangle\, \mathrm{d}x = 1$. Fig. 3 shows ϕ in the space-time map for $h = 2.5$. Note that the initial Gaussian bell shaped perturbation centered in $x = 1/2$ grows in space and time and requires less than 30 units of time to spread over all the spatial domain. Once the perturbation reaches the domain boundaries, it bounces back and oscillates with a constantly growing amplitude all over the domain. This kind of behavior is the signature of spatiotemporal chaos that takes place in all other solutions carried out, regardless the initial condition or mechanical energy level h.

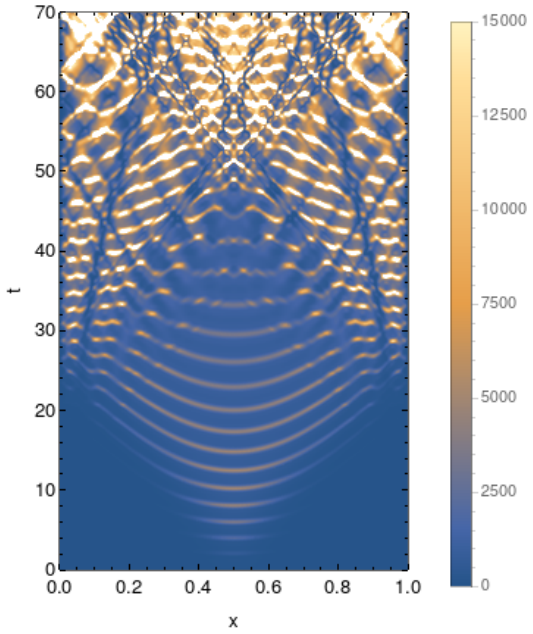

Figure 3. Perturbation analysis: ϕ spread in the space-time map for $h = 2.5$ and initial condition 1.

Due to the spatial homogeneous behavior of spatiotemporal chaos, one can employ Ψ as a parameter that quantifies the time evolution of the perturbation. Fig. 4a shows the evolution of the average of Ψ along time for various values of h. Note that during some initial transient time, the evolution Ψ is approximately the same for any h. After the transient, the lower h the lower is the slope assumed by the Ψ evolution. This slope is named herein as the perturbation growth rate. Moreover, after neglecting the first 2×10^4 transient time, the least square method is employed to fit the function $g(t) = \alpha\, t^{-1} + \beta\, t + \gamma$ to represent $(t, \log(\Psi))$ data. This nonlinear function captures the $\Psi(t)$ behavior for low levels of h. The derivative $g'(t)$ yields the perturbation growth rate, in such a way that at the limit $t \to \infty$, the growth rate neglecting any transient due to the effect of initial conditions: $\lim_{t\to\infty} g'(t) = \beta$.

Fig. 4b presents the coefficient β for all values of h, showing that higher levels of h that have an inter-well oscillation, presents a higher perturbation growth rate than for a intra-well oscillation. Besides, small variation of β is observed for the values of h which is characterized by inter-well oscillation. Based on that, one can infer that there is an upper limit of the perturbation growth rate, independently of the value of h. Additionally, the increase of σ increases the spatial coupling effect. For intra-well oscillations, the perturbation growth rate is higher for a higher σ, characterized by lower levels of h. On the other hand, an inter-well oscillation (achieved for higher level of energy h), the perturbation growth rate becomes smaller for higher σ.

4. CONCLUSIONS

This paper deals with spatiotemporal dynamics of Duffing-type systems governed by a partial differential equation (PDE). The PDE is solved by employing the Finite Difference Method for spatial discretization and fourth order Runge-Kutta method for temporal discretization. Numerical simulations regarding the system dynamical response show that, depending on the mechanical energy level of the system, the spatial mid point can display an intra-well or inter-well oscillation. Discrete Fourier Transformation is employed to help the comprehension of the system behavior. Perturbation analysis allows a proper comprehension of system dynamics. This analysis is performed by considering numerical simulations based on centered Gaussian initial perturbation that grows in both space and time continuously, characterizing

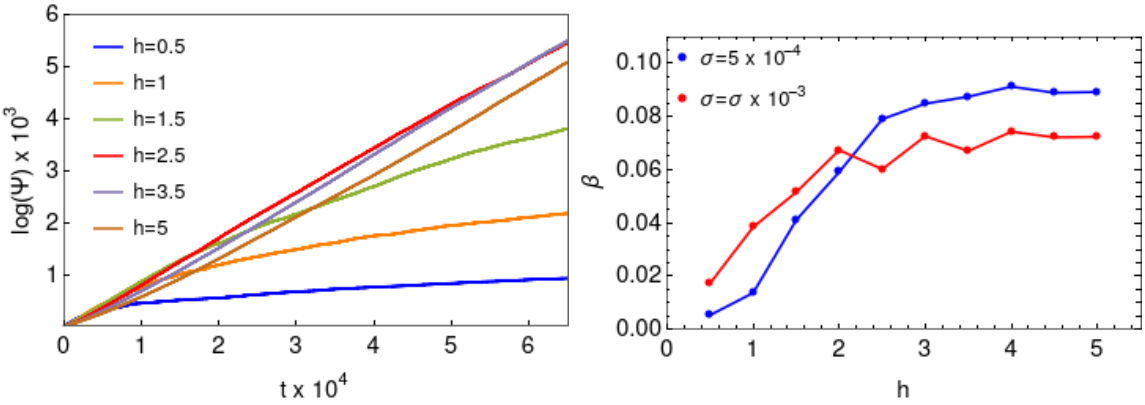

(a) Ψ along time for different energy levels h, and $\sigma = 5 \times 10^{-4}$ (b) Perturbation growth rate β at $t \to \infty$ as a function of h.

Figure 4. Perturbation evolution.

spatiotemporal chaos. The rate of the perturbation growth in time depends on the mechanical energy level of the system. For low levels, where the mid spatial point display an intra-well oscillation, the rate is lower than for higher levels, where the mid spatial point shows a inter-well oscillation.

5. ACKNOWLEDGMENTS

The authors would like to acknowledge the support of the Brazilian Research Agencies CNPq, CAPES and FAPERJ.

6. REFERENCES

Deissler, R.J., 1987. "Spatially growing waves, intermittency, and convective chaos in an open-flow system". *Pysica 25D*, pp. 233–260.

Deissler, R.J. and Kaneko, K., 1987. "Velocity-dependent Lyapunov exponents as a measure of chaos for open-flow systems". *Physics Letters A*, Vol. 119, No. 8.

Elder, K.R., Gunton, J.D. and Goldenfeld, N., 1997. "Transition to spatiotemporal chaos in the damped Kuramoto-Sivashinsky equation". *Physical Review E - Statistical Physics, Plasmas, Fluids, and Related Interdisciplinary Topics*, Vol. 56, No. 2, pp. 1631–1634.

Fang, X., Wen, J., Bonello, B., Yin, J. and Yu, D., 2017a. "Wave propagation in one-dimensional nonlinear acoustic metamaterials". *New Journal of Physics*, Vol. 19, No. 5, pp. 21–23.

Fang, X., Wen, J., Bonello, B., Yin, J. and Yu, D., 2017b. "Wave propagation in one-dimensional nonlinear acoustic metamaterials". *New Journal of Physics*, Vol. 19, No. 5.

Gotoda, H., Pradas, M. and Kalliadasis, S., 2015. "Nonlinear forecasting of the generalized kuramoto-sivashinsky equation". *International Journal of Bifurcation and Chaos*, Vol. 25, No. 5, pp. 1–19.

Guzmán, A.M. and Amon, C.H., 1994. "Transition to chaos in converging-diverging channel flows: Ruelle-Takens-Newhouse scenario". *Physics of Fluids*, Vol. 6, No. 6, pp. 1994–2002.

Hill, M., 1992. "Spatiotemporal chaos in the one-dimensional complex Ginzburg-Landau equation". *Physica D: Nonlinear Phenomena*, Vol. 57, pp. 241–248.

Merkin, J.H., Petrov, V., Scott, S.K. and Showalter, K., 1996. "Wave-induced chaos in a continuously fed unstirred reactor". *Journal of the Chemical Society - Faraday Transactions*, Vol. 92, No. 16, pp. 2911–2918.

Moon, F.C. and Holmes, P.J., 1979. "A magnetoelastic strange attractor". *Journal of Sound and Vibration*, Vol. 65, No. 2, pp. 275–296.

Musielak, D.E., Musielak, Z.E. and Benner, J.W., 2005. "Chaos and routes to chaos in coupled Duffing oscillators with multiple degrees of freedom". *Chaos, Solitons and Fractals*, Vol. 24, No. 4, pp. 907–922.

Reis, E.V.M., Sphaier, L.A., Nunes, L.C.S. and de B Alves, L.S., 2018. "Dynamic response of free span pipelines via linear and nonlinear stability analyses". *Ocean Engineering*, Vol. 163, No. January 2017, pp. 533–543.

Romeo, F. and Rega, G., 2006. "Wave propagation properties in oscillatory chains with cubic nonlinearities via nonlinear map approach". *Chaos, Solitons and Fractals*, Vol. 27, No. 3, pp. 606–617.

Umberger, D.K., Grebogi, C., Ott, E. and Afeyan, B., 1989. "Spatiotemporal dynamics in a dispersively coupled chain of nonlinear oscillators". *Physical Review A*, Vol. 39, No. 9, pp. 4835–4842.

Wackerbauer, R. and Showalter, K., 2003. "Collapse of spatiotemporal chaos". *Physical Review Letters*, Vol. 91, No. 17, pp. 31–34.

Yang, X.D. and Chen, L.Q., 2005. "Bifurcation and chaos of an axially accelerating viscoelastic beam". *Chaos, Solitons and Fractals*, Vol. 23, No. 1, pp. 249–258.

7. RESPONSIBILITY NOTICE

The authors are solely responsible for the printed material included in this paper.